IEEE Journal of Translational Engineering in Health and Medicine

Received 14 April 2025; revised 27 July 2025; accepted 6 August 2025.
Date of publication 8 August 2025; date of current version 14 August 2025.

Digital Object Identifier 10.1109/JTEHM.2025.3597088

Electroencephalography-Based Recognition of Low Mental Resilience Using Multi-Condition Decision-Level Fusion Approach

RUMAISA ABU HASAN[1], TONG BOON TANG[1], (Senior Member, IEEE), MUHAMAD SAIFUL BAHRI YUSOFF[2], AND SYED SAAD AZHAR ALI[3,4], (Senior Member, IEEE)

[1]Centre for Intelligent Signal and Imaging Research (CISIR), Universiti Teknologi PETRONAS, Seri Iskandar, Perak 32610, Malaysia
[2]Faculty of Medicine and Health Science, Universiti Putra Malaysia, Serdang, Selangor 43400, Malaysia
[3]Aerospace Engineering Department, King Fahd University of Petroleum and Minerals, Dhahran 31261, Saudi Arabia
[4]Interdisciplinary Research Center for Smart Mobility and Logistics, King Fahd University of Petroleum and Minerals, Dhahran 31261, Saudi Arabia

CORRESPONDING AUTHOR: T. B. TANG (tongboon.tang@utp.edu.my)

This work was supported in part by Malaysia Ministry of Higher Education (MOHE) through the Fundamental Research Grant Scheme under Grant FRGS/1/2021/TK0/UTP/02/25, and in part by the Higher Institution Centre of Excellence (HICoE) Scheme to Centre for Intelligent Signal and Imaging Research (CISIR).

This work involved human subjects or animals in its research. Approval of all ethical and experimental procedures and protocols was granted by the Ethics Committee of Universiti Pendidikan Sultan Idris under Application No. 2020-0121-01 and 2024-0256-01, and performed in line with the Declaration of Helsinki.

This article has supplementary downloadable material available at https://doi.org/10.1109/JTEHM.2025.3597088, provided by the authors.

ABSTRACT Background: Mental resilience is an important indicator of our defence mechanism against mental illness. The assessment of mental resilience is conventionally done using psychological questionnaires but more recently, has been investigated using neuroimaging modalities such as the Magnetic Resonance Imaging and Positron Emission Tomography. While having high spatial resolution, these modalities might not be cost-effective and accessible to serve larger populations. This pilot trial investigates the performance of electroencephalography (EEG) based system to assess mental resilience under different mental conditions. Methods: A total of sixty-eight healthy adults took part in this trial. Three types of EEG features, namely spectra, functional connectivity (FC) and effective connectivity (EC) were extracted, and their correlation with a standard resilience assessment instrument – the Connor-Davidson Resilience Scale were evaluated at resting and task conditions using stepwise regression. The features with the best goodness of fit model were then used to classify individuals into a low and high mental resilience class. Results: The EC features using phase slope index achieved the highest adjusted R^2 and the lowest root mean square error, compared to the spectral and FC features. The SVM classifiers trained with the EC features were able to recognize low mental resilience with accuracy at least 66% depending on the mental condition. Fusion of SVM scores from the eyes-closed, eyes-open and task conditions improved the classification accuracy to more than 85%. Conclusion: The pilot trial reveals the EC as the most promising EEG feature type in assessing mental resilience due to its measure of causality in brain activity, and demonstrates that the fusion of decisions among different mental conditions can help improve the recognition of low mental resilience. Findings from this trial contribute to maturing an EEG-based resilience assessment system development for workplace settings.

INDEX TERMS Effective connectivity, electroencephalography, mental resilience, neurotechnology.

Clinical Impact— Direct assessment using brain imaging modalities such as EEG provides a cost-effective means to assess mental resilience. To our knowledge, this is the first effort for healthy subjects. With the identified neuromarkers, the proposed solution demonstrates the potential to fuse EEG features from different mental conditions to provide accurate mental resilience assessment in workplace settings.

I. INTRODUCTION

MENTAL resilience is one of the defence mechanisms against mental illness. The emphasis on resilience came with the advocacy for prevention and wellness instead of the conventional risk-focused approaches in public health and clinical practices [1]. Resilience can be strengthened through social and cognitive reintegration as a person learns to adapt to future adversities [2]. Various training programs have been implemented to promote resilience in different cohorts, such as for working adults [3], athletes [4] and patients [5]. However, the current assessment of mental resilience is largely based on questionnaires [6]. These assessments define resilience as a set of stable personality traits or coping styles that allows a person to undergo positive growth following an adversity [7], [8]. The questionnaires can either directly measure resilience such as the Connor-Davidson Resilience Scale (CD-RISC) [9] and the Resilience Scale for Adults [10], or measure the associated factors of resilience such as hardiness, emotional intelligence and emotional coping strategies.

Phrased as an ordinary magic that is inherent in every person [11], the adaptation process of resilience against situations that can disrupt quality of life involves multiple systems such as genetic, biology and environment [12]. Neuroimaging modalities have been used to observe the neurophysiology of this adaptation process [13], [14]. The link between the brain and resilience often overlaps with findings from stress-related studies. Dai et al observed positive correlation between resilience and the habenula area, which is critical for emotional and stress processing [15]. Activation of the hypothalamus-pituitary-adrenal axis, which is a stress response pathway, during infancy (brain development) can influence the adaptation capacity against future life adversities [16], [17]. Compared to stress-related research, brain rhythms on mental resilience such as the alpha and beta oscillations are less explored in human subject research [18]. Researchers focused on structural and functional changes observed using modalities with high spatial resolution such as Magnetic Resonance Imaging (MRI) [15] and Positron Emission Tomography (PET) [19], [20]. With increasing evidence on the adaptive process observed during the fourth wave of resilience research [12], [18], [21], the electroencephalography (EEG) may pose as a good alternative to assess mental resilience due to its portability and high temporal resolution.

Moreover, there has been an increase in research interest in the mental resilience assessment in working adult population. The implications of work-related stress can lead to reduced quality of life and work productivity, and healthcare expenses which can cumulatively cost a person nearly $1200 per annum [22]. The work life of adults can be stressful since it demands them to face daily challenges which range from the physical nature of the job itself to the rapid changes in social and technical systems their workplaces. The increased awareness on mental health assessment has promoted the use of EEG to identify resilience in adults with stressful jobs such as teachers [23], construction workers [24], and nurses [25]. In addition to early screening for mental health conditions, these assessments may also provide physiological-based evidence for human resource management [26] and neuroergonomic design [27] which can contribute to nurturing a resilient workforce.

This work stems from the need to develop a neurotechnology solution to address the increasing workplace stress occurrence in adults. Current tools in the market are developed for stress response monitoring in non-clinical settings such as the Muse® and Neurosity Crown headsets. While they present stress related neuromarkers [28], it remains a challenge in assessing mental resilience [29], [30]. Hence, the purpose of our work is to address the challenge and demonstrate on how we can gain insight from quantifying the causal interaction of brain activities. This work also highlights shifts in effective connectivity underlying mental resilience as a person moves from resting to task condition, and that the fusions of these observations may improve assessment of mental resilience. Our findings provide evidence that mental resilience can be described by the adaptive interaction between multiple systems involving stimulus processing (external/ecological factor) and internal resources.

In summary, this paper presents a framework as a system to detect low mental resilience using EEG features at resting and task conditions. The pilot trial aims to assess the performance of the proposed system in identifying low mental resilience using EEG features extracted from different conditions of brain states. Spectral, functional connectivity (FC) and effective connectivity (EC) features are compared based on their predictive strength in estimating the resilience scores during resting and task conditions. Features with the best performance are then used to classify individuals into low or high mental resilience class. In this trial, we hypothesized that (1) the EC would perform better in predicting resilience scores due to its rich causality property in quantifying brain connectivity, and (2) the fusion of decisions based on EEG features extracted from resting and task conditions may improve the detection of low mental resilience.

II. METHODOLOGY

A total of sixty eight healthy adults were recruited as participants from two work settings: a postgraduate centre ($n_a = 43$, 22 females) and a childcare centre ($n_b = 25$, 24 females). The recruitment criteria for participants were healthy adults aged 18 and above, with normal or corrected-to-normal vision, and without hypertension, positive drug anamnesis, psychiatric diseases requiring inpatient treatment longer than two weeks, neurological disorders and malignant disease. Written informed consent to participate was obtained from each participant prior to the session. The pilot trial was conducted according to the guidelines of the Declaration of Helsinki, and ethical approval (reference no.: 2020-0121-01) has been obtained from the Ethics Committee of Universiti Pendidikan Sultan Idris.

The sample size was estimated at 5% type 1 error (α) using the formula for cross-sectional study design [31]

$$n = \left(\frac{Z_{\alpha/2}\sigma_x}{\delta}\right)^2 = \left(\frac{(1.96)(13)}{5}\right)^2 = 26 \tag{1}$$

where the population standard deviation σ_x and absolute error δ_x were extracted from the Connor-Davidson Resilience

Scale-25 (CD-RISC) questionnaire. The justification about the selection of the values is explained as follows. With a potential dropout rate of participants set to be 25%, the total subjects that were successfully recruited from the two centres were $n = 68$. Overall participants from the two centres had a balance ratio of males to females, albeit more males from the postgraduate centre and more females from the childcare centre. The Mann Whitney test was used to compare the age and resilience scores between the two centres.

The Connor-Davidson Resilience Scale-25 (CD-RISC) [9] was used to identify the resilience score of each participant. The questionnaire has 25 items with a 5-point Likert scale between the score 0 and 4. We used this 5-point scale to set $\delta_x = 5$ as the minimum precision needed to estimate the population resilience score. The total scores from these items can reach a maximum of 100 points with higher scores reflecting stronger resilience. In this trial, the score of 66 was used as threshold to label participants into low (LR) and high resilience (HR) classes. This threshold and σ_x used in equation 1 are computed as the pooled mean $\bar{X}_i$ and standard deviation s_i^2 of 24 studies reported in the CD-RISC manual [32], respectively, using the following equations [33]:

$$\text{Pooled Mean} = \frac{\sum(n_i - 1)\bar{X}_i}{\sum(n_i - 1)} \tag{2}$$

$$\text{Pooled standard deviation} = \sqrt{\frac{\sum(n_i - 1)s_i^2}{\sum(n_i - 1)}} \tag{3}$$

A. DATA COLLECTION

The experiment was conducted in a closed room with participant sitting on a chair whilst wearing an EEG cap. The EEG device used in this trial is the MITSAR-EEG-202-31 (Mitsar Ltd., St. Petersburg, Russia; certified with the IEC 60601-1 standard for medical electrical system) with 31 channels. To ensure optimal data recording, the impedance of EEG electrodes was kept below 10 kΩ. The EEG was recorded under both eyes-closed (CE) and eyes-open (EO1) resting conditions and during a mental imagery task with the Oculus Quest VR headset (as shown in Fig. 1). Participants were asked to sit on a chair calmly with minimal movement. Before the first task (Task1), the participants were asked to rest without the need to remove the VR headset. At this time, no audio or animated character was displayed through the VR headset. During the task, participants were presented with a virtual classroom where they were asked to perform a mental imagery task. The task were repeated twice (Task1 and Task2) with a 2-minute gap provided for the subjects to rest. After the task, the VR headset was removed and the participants were asked to relax with EO state (EO2) as the final block for the EEG recording. In summary, the entire protocol of EEG recording was 2-minute CE, 2-minute EO1, 4-minute Task1, 4-minute Task2 and 2-minute EO2, in sequence.

The mental imagery task was delivered to participants through a virtual environment. The environment was designed to emulate an early childhood education classroom

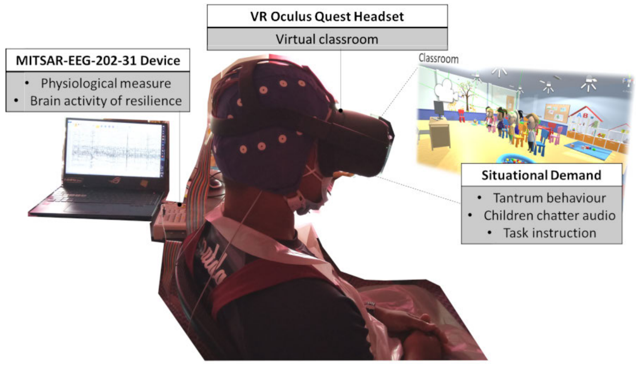

FIGURE 1. **Experimental setup with the 31 EEG cap and Oculus Quest headset during task condition. During the resting condition at the beginning and end of session, subject wore only the EEG cap for CE and EO states.**

with virtual children-characters programmed to exhibit tantrum behaviours throughout the four-minute class. This work setting was chosen as part of a longitudinal study to develop a resilience training module for early childhood educators that uses the VR and EEG technologies [23]. The classroom was programmed to mimic teacher-children interaction with audio and visual stimuli to emulate an actual children classroom. Each child-character in the virtual classroom was programmed to exhibit tantrum behaviours randomly throughout the class, which was then depicted with a red circle around the character. Throughout the task, the assumption was that the level of stress stimuli presented changes depending on the number of child-characters showing tantrum behaviour, as illustrated in Fig. 2. The participants were instructed to use their own mind strategy and imagery to calm the children.

B. FEATURE EXTRACTION

Brain signals were recorded using the EEG device at a sampling rate of 500 Hz using the 10-20 electrode montage. The right mastoid bone was set as the ground electrode and the left mastoid as the reference electrode. Firstly, the raw signals were filtered using the finite impulse response with a Hamming-sinc window to obtain oscillations between 1 Hz and 45 Hz. Channels with a power spectrum larger than three standard deviations from the average power spectrum of 31 channels were labelled as bad channels. Artefacts were removed using the wavelet thresholding method in the HAPPILEE toolbox [34]. The EEG signals were transformed using the biorthogonal wavelet `bior4.4` (decomposition level = 9) to extract wavelet coefficients. These coefficients were then thresholded using a Bayesian denoising method, with `hard` threshold rule and `level-dependent` noise estimation parameters. Those frequency components with their coefficients identified as artefacts were converted back into time series via inverse wavelet transform and subtracted from the original EEG signals. This method has the advantage of removing artefacts without the reduction of timepoints, which is crucial for low-density EEG.

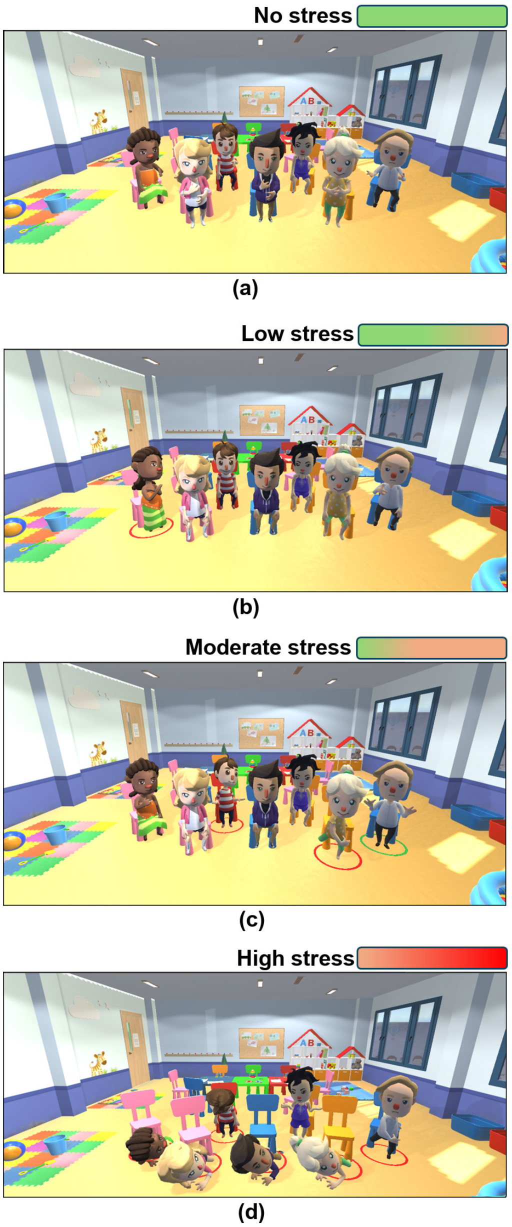

FIGURE 2. Changes in the VR environment from absence to high stress stimuli (a-d) throughout the mental imagery task. Tantrum behaviours were accompanied with a red circle displayed around the child-characters. Green circle indicates a positive interaction exhibited by the child-characters to emulate communicative gesture.

Independent Component Analysis (ICA) was conducted by using the extended `Infomax` algorithm to categorize the independent components (ICs) into seven classes based on physiological activity (brain, heart, eyes, and muscle) and environmental artefacts (line, channel and indeterminant noises) [35]. For each IC, the `IClabel` function estimates the probabilities across all seven classes and subsequently label it based on the highest probability. Only ICs labeled as brain activity were retained to reconstruct the clean EEG signals. Bad channels were then interpolated from neighbouring channels using spherical interpolation.

To address volume-conduction effect in EEG studies, source localization issue must be taken into consideration in the preprocessing steps to ensure minimal mixing of uncorrelated sources. The two main categories of source localization solution are sensor-space and source-space methods. Surface Laplacian is a reference-independent method of sensor-space localization that transforms the EEG signals into estimates of current sources/sinks at the dura layer known as the current source density (CSD) [36], [37]. Although its topological distribution may be less interpretable to the deeper brain sources, the method relies on lesser parameters and assumptions such as the inter-electrode distance and spline factor to improve spatial resolution and address drawbacks of volume conduction effects in EEG signals [38]. The method has been observed to deliver reliable findings in both clinical and developmental cohorts [39]. In this study, we used the spherical laplacian method by Perrin et al. [40] implemented in [37] where the spline flexibility is set to $m = 4$, and the G smoothing parameter is set to $\lambda = 1e^{-5}$.

Under all task conditions, data from only the first two minutes were analysed for feature extraction to ensure consistent length of time under the CE, EO1, EO2 conditions. Three types of EEG features (spectral, functional connectivity and effective connectivity) were extracted to analyse the brain activity of resilience in eight frequency bands: delta (1)-4 Hz), theta (4)-8 Hz), alpha1 (8-10 Hz), alpha2 (10-13 Hz), beta1 (13-15 Hz), beta2 (15-20 Hz), beta3 (20-30 Hz) and gamma (30-45 Hz). Extraction of the features from each subject resulted in three vectors of different feature types: Spectra (1×248), phase-locking value or PLV from functional connectivity analysis (1×3720) and phase slope index, PSI from effective connectivity analysis (1×3720).

Firstly, spectral features were computed using the Welch's method. The Welch's method segments the EEG signal with an overlapping window function. To calculate the power spectral density of an EEG signal, let X_n be a sample of the signal with segments of the signal are defined as

$$X_1(n) = X(n), X_2(n) = X(n + D) \tag{4}$$

where L is length of segment. This results in sequence of

$$X_k(n) = X(n + iD) \text{ segments} \tag{5}$$

where $i = 0, \ldots, K-1$ and K is the total number of segments. The offset distance D is set to 50% overlap. In the EEG signal, $X_k(n)$ is the time-series of single channel. A data window, $W(n)$, is used to form sequences of windowed data segments defined as $X_k(n)W(n)$. Discrete Fourier Transform is used to calculate K number of modified periodograms

$$P_k(f) = \frac{1}{LU}\left|\sum_{n=0}^{L-1} X_k(n)W(n)e^{-i2\Pi fn}\right| \tag{6}$$

where $k = 1, 2, \ldots, K$ and U is a constant of the Hamming window function. The Welch's spectral estimate is then computed as the average of $P_k(f)$, giving

$$\hat{P}_W(f) = \frac{1}{K}\sum_{k=1}^{K} P_k(f). \tag{7}$$

In computing the Welch's spectral value, longer L can lead to noisy PSD due to smaller number of segments; smaller window length will result in a smooth PSD but with a poor frequency resolution. Therefore, there needs to be a balance in the window length and percentage of overlapping to ensure an optimal number of segments to compute the PSD [41]. As the lower limit of delta brainwave is 1 Hz, the window length needs to be $L > 2/f_{low}$ seconds to ensure at least two full cycle of the 1-Hz delta oscillation [42]. In this trial, a 4-second window length was chosen with 50% overlap [43]. Relative power was calculated as the ratio of absolute power to the total power of the whole frequency range of 1-45 Hz.

$$\text{Relative power} = \frac{\text{Absolute power}}{\text{Broadband power}} \tag{8}$$

Secondly, the FC features were extracted using the phase-locking value (PLV) metric [44]. The PLV is computed from the difference in instantaneous phase between two signals. This metric does not apply the approach of non-zero-phase only, and therefore has been inferred as having a poor volume-conduction sensitivity. However, not all zero-phase differences result from the linear mixing of volume-conduction. These components may reflect delay in long-range synchronization [45], [46]. Moreover, the PLV is robust against amplitude fluctuations in time series, and captures the temporal synchrony in the non-linear EEG signals [47]. Paban et al reported negative correlation between resilience scores and graph-based flexibility derived from the PLV [48]. Hence, the PLV is selected as the FC feature to be analysed in this study. Signal from each channel $X(n)$ was undergone Hilbert transform to produce a signal,

$$X_{an}(n) = X(n) + jX_H(n). \tag{9}$$

The instantaneous phase of $X_{an}(n)$ can then be computed as

$$\phi_{X_{an}}(n) = tan^{-1}\frac{X_H(n)}{X(n)}. \tag{10}$$

The synchronization between two signals from channel $X(n)$ and $Y(n)$ can be measured as the phase difference:

$$\delta\phi_{XY}(n) = \left|\phi_{X_{an}}(n) - \phi_{Y_{an}}(n)\right|. \tag{11}$$

Therefore, the PLV is computed as the summation of phase differences divided by N number of datapoint [41], as in

$$PLV_{XY} = \frac{1}{N}\left|\sum_{n=1}^{N} e^{j\delta\phi_{XY}(n)}\right|. \tag{12}$$

The PLV was computed and averaged across the 1-minute segment to obtain an index within the range of [0,1]. Length of the window depended on the central frequency of each bands, and computed as $\frac{6}{centralfrequency}$ [48], [49]. Larger PLV indicates that the phase differences between the two signals remained highly synchronized across the time series [41]. A close-to-zero PLV reflects a poor synchronization and the $\delta\phi_{XY}(t)$ is distributed across the unit circle of $[0,2\pi]$ phase interval.

The third type of EEG feature extracted is the phase slope index (PSI) – a measure of EC. The PSI carries information of directional connectivity between pairs of electrodes. It is extracted from the imaginary part of coherence and therefore removes components with zero-phase difference associated with the linear mixing of uncorrelated nearby sources [50]. This EC measure retains only the neuronal interactions with truly phase-lagged connectivity and therefore is robust against the instantaneity and periodicity of field spread due to volume conduction. Comparative analysis between EC measures have reported PSI to be more robust against volume conduction and SNR drop, and was able to detect more causal connections and lesser non-causal connections [51], [52], [53]. Continuous EEG signal is segmented into K segments of duration T with 50% overlap. The coherency, C_{ij}, between channel i and j is computed from the estimated cross-spectral density S_{ij} as

$$C_{ij} = \frac{S_{ij}(f)}{\sqrt{S_{ii}(f)S_{jj}(f)}}. \tag{13}$$

The PSI, $\tilde{\Psi}_{ij}$, is defined as the imaginary part of C_{ij} [51]

$$\tilde{\Psi}_{ij} = \Im\left(\sum_{f\in F} C^*_{ij}(f)C_{ij}(f+\delta f)\right) \tag{14}$$

where the frequency resolution is $\delta f = 1/T$. Similar to the computation of spectral and PLV features, the PSI was calculated for 1-minute segments of the CSD-transformed signals [54]. For each one-minute epoch, it was segmented with 50% overlap into 4-second segments. This measure has been reported to be robust against mixture of signal sources due to volume conduction [51], [55]. For both FC and EC features, the strength of each nodes contributing to the brain synchronization can be computed as the nodal strength (st_{in} and st_{inout}), which is the sum of inward and outward links through a node [56].

C. DATA ANALYSIS

In this paper, the EEG signals were analysed in two phases. The first phase involves comparing the linear regression models between the three types of EEG feature. A stepwise linear regression was conducted to compare the coefficient of determination (R^2) and root-mean-square-error ($RMSE$) between models. Each potential predictors from the three feature vectors were tested for normality using the Shapiro-Wilk test, and for potential association using the Pearson correlation coefficient. Outliers were excluded based on the scaled median absolute deviation criterion defined as 15 where b is the constant for normality assumption and A is the set of observation [57].

$$MAD = b \times median(|A - median(A)|) \tag{15}$$

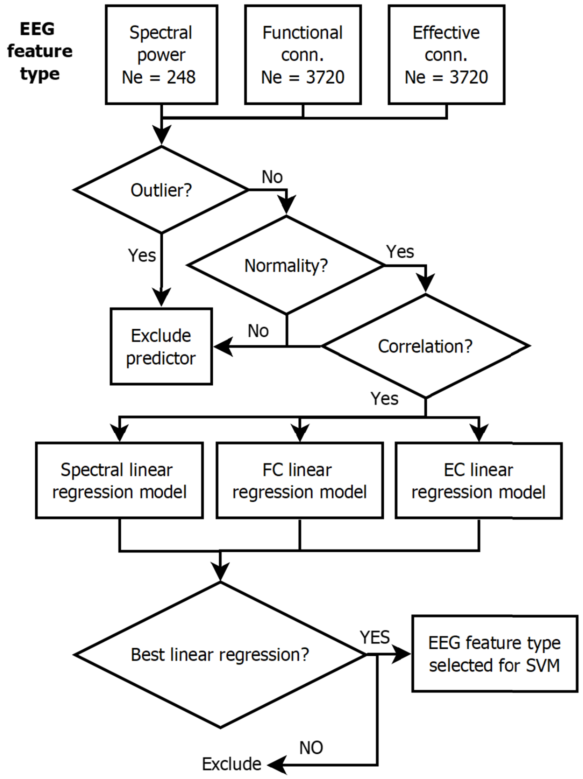

FIGURE 3. Phase 1: Selection of predictors for each EEG feature to be entered into the stepwise regression models. Notes- Ne: Number of extracted predictors.

Following the one-in-ten rule of thumb in regression modeling, the maximum number of predictors accepted is set to be six ($n_{subject} = 68$) to ensure a good fit model and avoid potential overfitting issues. Durbin Watson statistic and Shapiro-Wilk test were used on each regression model to test for auto-correlation of predictors and normality of residuals, respectively. Figure 3 illustrates the process of excluding the predictors for the regression model and selecting the best EEG feature type. In the second phase, the selected EEG feature type is then used to train a classification model to detect high and low resilience groups.

D. MULTI-CONDITION DECISION-LEVEL FUSION

For the classification model, the dataset was split with a 90-10 ratio for training ($n = 61$) and testing ($n = 7$), respectively. Spearman correlation test was used to select significant features with $p < 0.025$. Figure 4 presents the whole framework implemented to build the low mental resilience recognition system. Linear support vector machine (SVM) classifier was used to build the singular classification model for each mental condition, as this classifier has been reported to achieve good classification performance in identifying EEG neuromarkers for stress [58], emotion [28], pain [59], and vigilance [60]. The models were trained using a nested Leave-One-Out-Cross-Validation (LOOCV) approach. For each fold, the classification loss was calculated based on

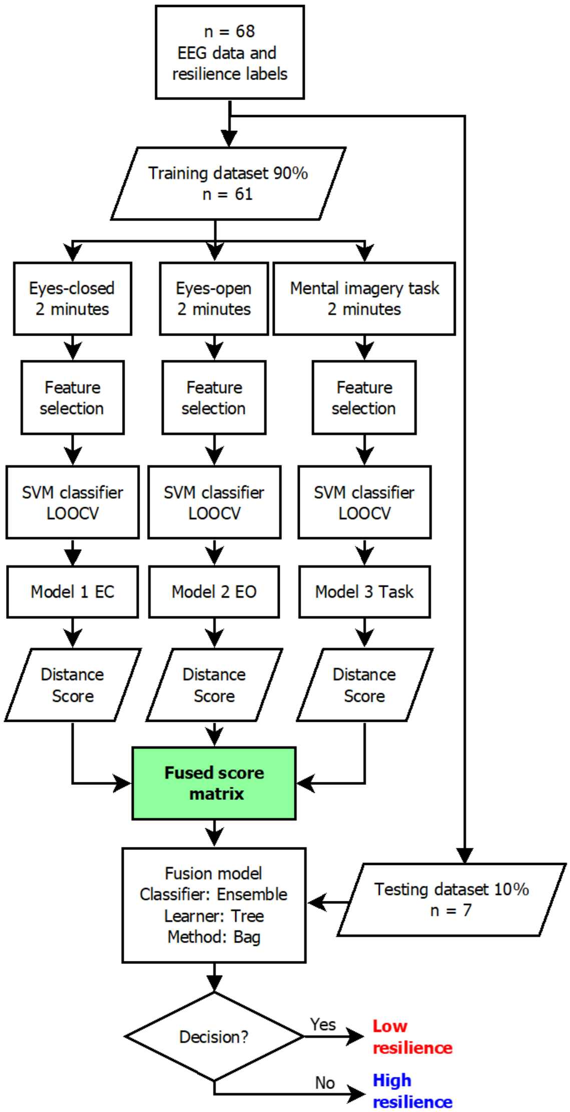

FIGURE 4. Phase 2: Framework to detect low mental resilience using multi-condition decision-level fusion approach.

the inner-fold observations using the model trained on the outer-fold observation. Kernel scale and box constraint hyper-parameters were tuned for optimization using the Bayesian expected-improvement acquisition function, with the maximum number of objective function evaluations set to be 30. Classification loss from each fold was then averaged across the LOOCV fold to compute the classification accuracy of the model. The accuracies were compared between mental conditions to select the three best models comprising CE, EO and Task conditions. For each observation, the SVM model computes two distance scores that measure the signed distance ($\pm d_x$) between the observation x_n and the decision boundary, for each class. The scores can range between $(-\infty, +\infty)$ where the model will classify the observation into the class yielding positive distance score. The Wilcoxon rank sum test was conducted to compare the differences in distance scores between the LR and HR classes.

IEEE Journal of Translational Engineering in Health and Medicine

Since the distance scores for both classes have the same magnitude but with different signs (e.g., $d_{x_{\text{Class1}}} = -1.463, d_{x_{\text{Class2}}} = 1.463 \therefore x_{\text{predicted}} = \text{HR class}$), only one distance score vector was selected from each CE, EO and Task models as input for the fusion model and thus, resulting in an $n_{\text{training}} \times 3$ matrix. The fusion model was trained using the Ensemble classifier with decision-tree as the weak learner/base model, and bagging aggregation method. The LOOCV approach was used to tune the hyper-parameters of the fusion model: the number of learning cycles, minimum number of leaf node observations and maximum number of splits. Performance was evaluated using accuracy, precision, sensitivity, specificity and F-measure metrics. Predictor importance was also estimated by summing the changes in nodal impurity due to splits caused by each predictor and dividing it by the total number of branch nodes. Estimates from each weak learner were then averaged to compare the importance between the three mental conditions.

III. RESULTS

Analysis on the demography of participants between the two recruited centres revealed similar levels of resilience scores (postgraduate: 68.63 ± 10.77, childcare: 68.32 ± 10.41, $p = 0.78$) but with significantly different age range (postgraduate: 24.92 ± 4.69, childcare: 33.52 ± 5.52, $p < 0.01$). A post-hoc analysis conducted by using the Spearman's rho coefficient on the potential relationship between age and gender, and resilience showed weak correlation (age: $rho = -0.04$, $p = 0.91$; gender: $rho = -0.21$, $p = 0.09$). These results suggest that the participants had similar level of resilience despite having different work experience and age. The whole cohort ($n = 68$) had a mean age of 28.42 ± 6.58 and an average CD-RISC score of 68.51 ± 10.56. Thirty subjects were labeled as low-resilient (59.57 ± 4.61) and 38 subjects were labeled as high-resilient (75.58 ± 8.32).

A large number of features were excluded as potential predictors for the regression model due to being outliers, having no correlation with the CD-RISC scores or in non-normal distribution. The number of potential predictors entered for each respective models based on the EEG feature type were larger for the EC ($n_{ec} = 51$, $n_{eo1} = 47$, $n_{eo2} = 52$, $n_{task1} = 61$, $n_{task2} = 66$), as compared to the FC ($n_{ec} = 37$, $n_{eo1} = 26$, $n_{eo2} = 17$, $n_{task1} = 16$, $n_{task2} = 21$), and spectral power ($n_{ec} = 0$, $n_{eo1} = 15$, $n_{eo2} = 2$, $n_{task1} = 6$, $n_{task2} = 16$).

Table 1 presents the regression models for each EEG feature and mental condition. All models had normally distributed residuals ($p_{\text{residual}} > 0.05$) and no autocorrelation between the predictors ($p_{\text{durbin}} > 0.05$). The EC models predicted resilience scores with the lowest *RMSE* values and the largest adjusted R^2, as shown in Figure 5. The low R^2 of the spectral models was expected since only one feature was extracted to explain the variance in resilience scores. Meanwhile, the FC models had lower adjusted R^2 than the EC despite having similar n_p for the eyes-open and task conditions. This suggests the EC as a better EEG feature type to detect low mental resilience level and therefore is a preferred choice for such binary classification models trained in Phase 2.

From a total of 3720 extracted EC features, predictors to the SVM classification model were reduced to a subset of features (n_{p2}) based on their correlation to the CD-RISC scores. Table 2 tabulates the number of predictors and accuracy of each SVM classification model based on the mental conditions. The conditions for CE, EO2 and Task2 resulted in better classification accuracies and therefore were selected for the multi-condition decision-level fusion. These three conditions

TABLE 1. Regression models of each EEG feature based on different mental condition.

Condition	Feature	Spectral	FC	EC
CE	n_{p1}	0	3	6
	$F(df1, df2)$	-	10.56 (3,62)	19.14 (6,59)
	p_{durbin}	-	0.97	0.25
	$p_{residual}$	-	0.29	0.74
EO1	n_{p1}	1	6	6
	$F(df1, df2)$	9.53 (1,64)	10.42 (6,59)	12.86 (6,59)
	p_{durbin}	0.49	0.57	0.30
	$p_{residual}$	0.16	0.36	0.91
EO2	n_{p1}	1	6	6
	$F(df1, df2)$	7.54 (1,61)	9.56 (6,56)	15.74 (6,56)
	p_{durbin}	0.98	0.86	0.45
	$p_{residual}$	0.24	0.69	0.68
Task1	n_{p1}	1	5	6
	$F(df1, df2)$	9.76 (1,62)	9.72 (6,57)	18.23 (6,57)
	$durbin$	0.96	0.27	0.22
	$p_{residual}$	0.76	0.83	0.43
Task2	n_{p1}	1	6	6
	$F(df1, df2)$	14.85 (1,58)	11.63 (5,54)	16.29 (6,53)
	p_{durbin}	0.19	0.58	0.79
	$p_{residual}$	0.02	0.24	0.53

Notes: FC - functional connectivity; EC - effective connectivity; p_{durbin} - p-value for Durbin Watson statistics; $p_{residual}$ - p-value for normality of residuals; n_{p1} - numbers of predictor selected for Phase 1.

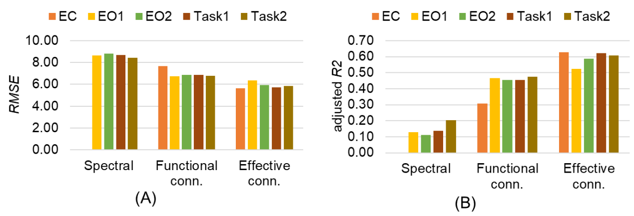

FIGURE 5. Performance of the regression models based on (A) *RMSE* and (B) R^2. The low *RMSE* and high adjusted R^2 observed in the EC models suggest better predictive strength (adjusted R^2 > 0.5) in estimating the CD-RISC scores.

TABLE 2. LOOCV accuracy of the SVM classification models based on EC features.

Condition	n_{p2}	Accuracy (%)	Selected for fusion
CE	99	75.41 ± 43.42	✓
EO1	76	73.77 ± 44.35	
EO2	87	81.03 ± 39.55	✓
Task1	80	67.80 ± 47.13	
Task2	84	83.64 ± 37.34	✓

Notes: n_{p2} - numbers of predictor selected in Phase 2.

TABLE 3. Performance of the fused-classification model.

Performance	LOOCV (%)				Testing (%)
	CE	EO	Task	Fused	
Precision	75.11	84.97	83.60	88.31	87.5
Sensitivity	74.89	78.48	83.69	88.56	87.5
Specificity	74.89	78.48	83.69	88.56	87.5
Accuracy	75.41	81.03	83.64	88.52	85.71
F-measure	74.98	79.25	83.61	88.41	85.71

are referred onwards as CE, EO and Task. The EC features selected ($\sum n_{p2} = 270$) are illustrated in Fig. 6 where the arrow width reflects the correlational strength between the EC and mental resilience score. Connections with wider arrows show stronger correlation with the CD-RISC scores whereas thinner arrows indicate moderate correlation ($p < 0.025$). The connections were found to be mostly unique to the respective SVM models, with 250 predictors were exclusive to a specific mental condition and brainwave. Only 10 predictors were selected twice for different mental conditions as shown by the red arrows in Fig. 6. These repeated predictors were mainly within the high frequency brainwaves between alpha2 and gamma oscillations. Further details on the 270 EC features selected as predictors are given in the Supplementary files.

Nodal analysis on the inward and outward strengths of the EC predictors illustrates the causal differences between the LR and HR classes. The LR class has an inward strength $st_{in} = [0.50,3.81]$ and $st_{out} = [-5.24, -0.87]$ whereas the HR class has $st_{in} = [0.06,4.27]$ and $st_{out} = [-2.74, -0.51]$. On average, the LR class transmits more information than the HR class whilst the latter receives more information across mental condition and brainwaves. The regions involved in these information flux are also different, as shown in Fig. 7. Yellow regions indicates stronger inward links and reception of information, whereas red regions show stronger outward links and transmission of information. Differences can be observed in the laterality in frontal and parietal regions, and the occipital cortex. The LR class sends more information in the right frontal area an left parietal region whereas the HR class receives more information from these regions. The outward flux in HR class were also higher in the visual cortex, which highlights the role of eyes-open during both resting and task conditions.

From the CE, EO, and Task models, the distance scores, $d_{x_{Class1}}$ and $d_{x_{Class2}}$ computed by the SVM classifiers were fused and trained using the Ensemble classifier. These scores were significantly different between the two resilience classes as shown in Fig. 8. The LR class had significantly higher scores for $d_{x_{Class1}}$ whereas the HR class had significantly higher scores for $d_{x_{Class2}}$ across the three models. The fusion of decisions from multi-condition resulted in a higher accuracy as shown in Table 3. The performance matrix of the fused model were higher and more stable than the LOOCV models of EC, EO and Task conditions. Fig. 9 presents the confusion matrix of both the LOOCV and test performance for the fusion model. Analysis on the importance of distance scores as predictors to the fusion model in Fig. 9(C) reveals higher contribution from the Task condition. The order of predictor importance also conforms to the LOOCV performance of the SVM models where Task condition resulted in the best performance in terms of sensitivity, specificity and accuracy. The EO condition achieved similar accuracy but has a drop in sensitivity and specificity performances.

IV. DISCUSSION

A. NOVELTY OF THIS WORK AND RELATED LITERATURE

This pilot trial hypothesized that the EEG might be a suitable tool to assess mental resilience. More specifically, the EC would perform better in predicting mental resilience due to its rich causality property in quantifying brain connectivity. Comparison result among the EEG features shows that the EC features outperformed the spectral and FC features in predicting resilience during resting and task conditions ($R^2{}_{\text{adj}} > 0.5$). To the best knowledge of the authors, this is the first study that compares different EEG features as potential neuromarkers of mental resilience. To date, the understanding about the brainwaves underlying mental resilience is limited by the number of studies conducted on mental resilience. The findings from such studies are often integrated with a view that the absence of illness is a sign of resilience [18]. Kalisch et al highlighted the need to differentiate between mental resilience and vulnerability against pathophysiology conditions [61]. Moreover, the diversed understanding about resilience reflects the need to observe resilience within the context of population and culture [62]. In this trial, the findings of EEG features are within the context of healthy and working adults and therefore infers on the mental resilience of a healthy brain.

There are several EEG studies that analyse the spectral features associated with mental resilience. In a study involving children with maltreatment history, alpha asymmetry predicted their resilience with moderate effect size. Those with higher alpha asymmetry across the C3-C4 homologous pair were more likely to have higher resilience scores [63]. This relationship however, weaken when the prediction model had maltreatment status and emotion regulation as predictors. Adults practising sedentary lifestyle and had low resilience scores exhibited higher theta, alpha and beta1 brainwaves at the frontal gyrus [64]. Similarly, changes in spectral power due to the Flaker Task examining resiliency against distractors that predicted the resilience scores were only observed in the alpha brainwaves and not in theta and beta brainwaves [65]. However, another study reported no significant difference between low and high resilience groups in the alpha and beta asymmetries at rest [29]. KeunhoYoo et al. also reported no significant correlation between resilience and the spectral powers at resting [30]. These findings may reflect the limitations of spectral feature in assessing the complexity of mental resilience since this EEG feature quantifies localized rhythmic brain activity but not the changes in regional (such as FC and EC) or temporal brain activity.

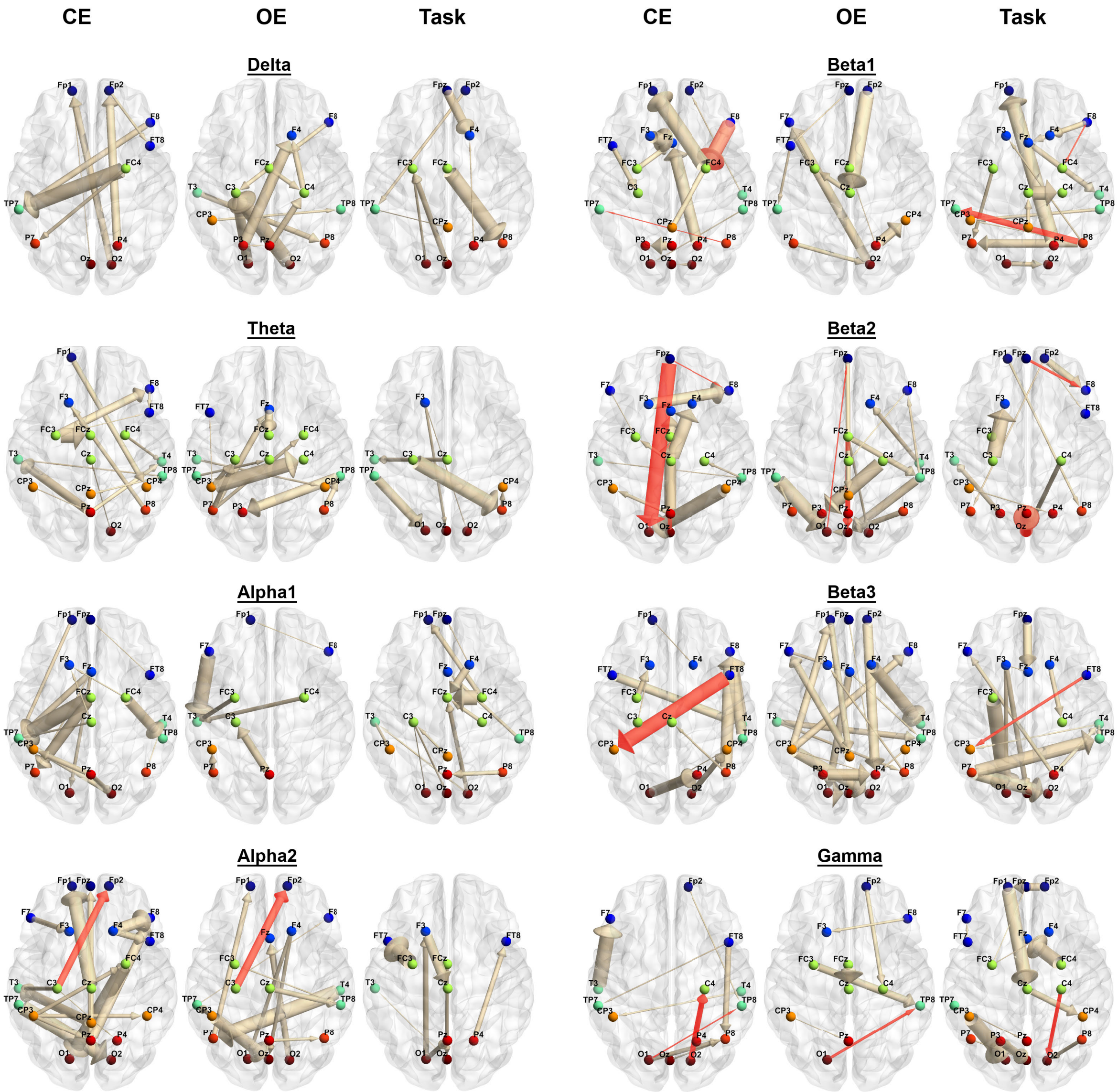

FIGURE 6. **EC predictors of resilience based on the CE, EO and Task conditions, and frequency brainwaves. Directional arrow display the causality of EC between two nodes and the arrow width reflects the correlation strength ($p < 0.025$) between the EC and CD-RISC scores. The predictors are largely unique to each mental conditions and brainwaves with only 10 connections (red arrow) repeated in either two mental conditions.**

There has been an increase in brain connectivity research on mental resilience. The relevance of studying brain network conforms to the shift in resilience concept as the adaptive mechanisms between multiple systems [12]. The network architecture associated with a healthy brain can be used as the benchmark for mental resilience, where deviations in the network metrics may reflect at-risk or pathological conditions [61], [66]. Brain networks generated from FC have been used to compare the network property between clinical and healthy cohorts that differentiates the resiliency against diseases [67], [68], [69]. Compared to the FC, the study of causality in brain activity of mental resilience defined by EC is still growing.

The poor performance observed in the spectral and FC models emphasize the role of synchronous and desynchronous brain activation related to mental resilience. Effective connectivity measure the synchronization and direction of information between brain regions. A study on the associated factors of resilience used the directed transfer function to conduct binary classification between four groups of emotion regulation strategies [70]. The EC was used to extract six graph theory metrics as predictors to the deep learning model and achieved prediction accuracy greater than 90% when used features from broadband, beta and gamma brainwaves with eyes-closed resting condition. The causality of brain pathways and connectivity underlying resilience and

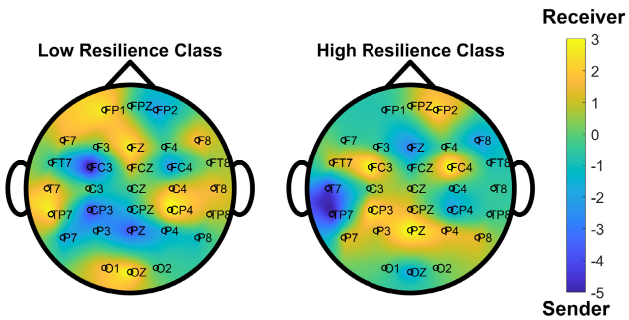

FIGURE 7. **Differences in the averaged inward (yellow) and outward (blue) strength between (A) LR and (B) HR classes. The LR class receives more information in the left frontal and right parietal areas whereas the HR class receives more information in the right frontal and central parietal areas. The latter also transmits more information from the visual cortex compared to the LR class.**

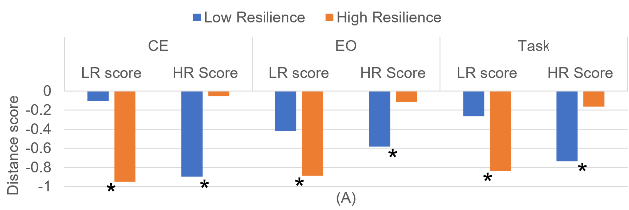

FIGURE 8. **Comparison of the distance scores between the LR and HR classes for CE, OE and Task SVM models. Significant differences were observed ($p < 0.05$) for all six distance scores where $d_{x_{Class1}}$ is positive in the LR class whereas $d_{x_{Class1}}$ is positive in the HR class. A positive score indicates that x is on the same side of the respective class with reference to the decision boundary, and therefore is the predicted class.**

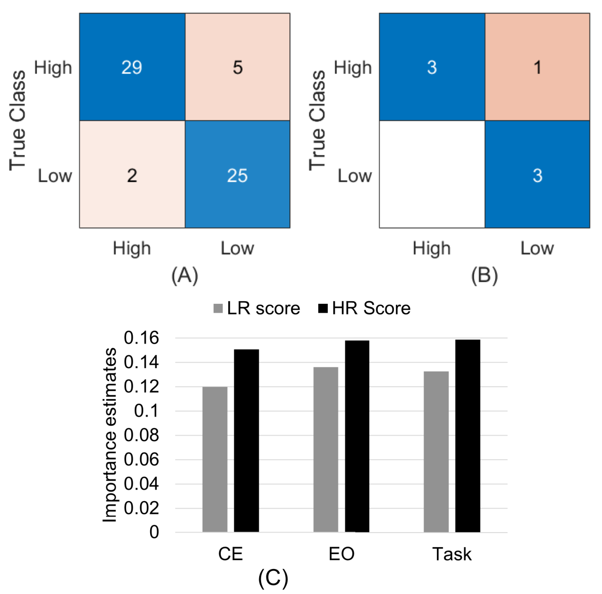

FIGURE 9. **Confusion matrix for the (A) LOOCV and (B) testing performances of the fused model, and the (C) estimated importance of the SVM classification scores used as the fused features for the Ensemble model.**

its responses towards stress has been documented in both animal and human subject research, where the structural and functional changes in the brain since early development can either protect against or cause vulnerability towards pathophysiological changes [13], [16], [71]. These findings highlight the strength of EC in assessing mental resilience in both healthy and clinical populations.

Findings from this trial show that this EEG feature type can be a strong neuromarker in assessing different levels of resilience. The poor performance of the FC may indicate that the current framework is not suitable to extract the PLV metric for resilience assessment. This was also observed in [48] where the brain network extracted from static PLV metric did not correlate with CD-RISC scores whereas the dynamic PLV metric observed significant correlation in the delta, alpha and beta brain networks. A comparative analysis of the predictive strength between effective and FC in assessing MDD patients and healthy cohort also reported the former achieving 91.67% accuracy with 19 features, and the latter achieving 89.36% accuracy with 6650 features [72]. The PSI measure selected as the EC measure in this work has also been used in resilience-related studies such as intelligence [73], mild cognitive impairment [74] and emotional perception [75]. An empirical study comparing three EC to classify emotional states reported that the PSI performed better than the directed transfer function and generalized partial directed coherence measures [75]. This may be attributed to the PSI being less dependent on the linear relationship between pairwise signals [76]. In the current work, the FC features were largely excluded from being potential predictors due to non-significant contribution to the regression model and the drop in predictive performance reflected in the adjusted R-squared and model residuals.

B. BIOLOGICAL INTERPRETATION ON THE IDENTIFIED NEUROMARKERS

The inward st_{in} and outward st_{out} strength were observed to have opposite pattern between the LR and HR groups where they had stronger st_{out} and st_{in}, respectively. This suggests that the LR group had more nodes that acted as transmitters whilst in the HR group, more nodes were acting as receivers. The information flowing within a brain network carry excitatory-inhibitory inputs from and to specific brain regions to maintain a healthy brain architecture. The differences between the LR and HR groups were largely observed in the central parietal region, frontal region and the visual area. The fronto-parietal network, also known as the central executive network, regulates top-down attentional control and goal-directed behaviour [77]. It is responsible in selecting or suppressing information based on relevance, allowing inhibitory control against impulsive reaction to execute goal-directed behaviour. The high outward flow of information observed in the LR group in the central parietal region may reflect lower inhibitory control in regulating top-down cognition. This can lead to a person adopting a poorer strategy against a conflict due to excessive monitoring of thoughts and behaviour [78].

These regions have also been reported in studies related to emotional and cognitive processing. The increased in brain synchronization in the frontal-parietal regions observed in healthy aging population reflected preservation of cognitive function [69]. Lifetime experience in both adults and pediatric populations influenced the event-related responses in the left parietal region [79]. In the resting study on mental resilience using dynamic PLV, Paban et al. [48] reported high correlation between resilience score and the source-space localized brain activity in the left caudal anterior cingulate region, which is located near the fronto-temporal area on the scalp. These regions are involved in establishing efficient global communication of the brain, especially in the cognitive regulation of behaviour [48]. Asymmetrical activities measured from these regions have also predicted different emotional states of neutrality, fear, sadness and happiness [80]. In a recent study, spectral comparison between low and high resilience groups reported significant differences observed in the alpha activity in the anterior midlines and parietal regions, and the right frontal and central regions [81]. The laterality in frontal and parietal regions were also observed in our study between the two classes. The LR class had more laterality where the left regions were transmitting more information and the right regions had more inward links. Meanwhile in the HR class, the inward and outward links reflecting reception and transmission of information were more bilateral, suggesting better recruitment of brain regions and cognitive performance [69].

Moreover, the differences in information flow at the left and right prefrontal areas between the two groups implicate the role of emotional regulation associated with mental resilience. Asymmetrical brain activity in the left or right prefrontal areas has been linked to avoidance or approach-oriented behaviours, respectively [82]. Larger right prefrontal structures have been associated with positive adaptation in mental resilience [83]. Low resilient adults have been associated with shrinkage of dendrites in some regions of prefrontal cortex and reduced functional connectivity [13]. On the neurobiological level, the brain mechanisms of resilience have been observed in neural pathways such as the hypothalamic-pituitary-adrenal axis within the neuroendocrine system, hippocampus, medial prefrontal cortex and the reward pathway responsible in the regulation of dopamine on the cellular level and goal-directed behaviours [16]. Hence, this study provides evidence from the perspective of sensor-space EEG analysis that corroborates with the observations reported in previous literature.

Another significant difference observed between the two groups is near the T7 and TP7 areas, which represent the left temporoparietal junction at cortical level. This junction has been associated with the "theory of mind" which is the ability to perceive self-to-others' differences in belief, intention and desire [84]. This process promotes mental state reasoning and constitutes both social perception (low-level) and social reasoning (high-level) functions. The high outward flow observed in the HR group at this junction may reflect mental state reasoning which leads to contextual updating between internal and external resources in the brain based on the most relevant information to formulate appropriate behavioural responses [85]. In psychological instruments, this ability can be linked to mental resilience factors such as having a secure relationship and spirituality [9].

C. DYNAMICS OF MENTAL RESILIENCE

According to the transactional model of stress, the four major elements needed to elicit emotional resilience are situational demands, physiological arousal responses, cognitive appraisal of the situation, and instrumental and coping behaviour [86]. Through learning and adaptation, the pattern of information flow in the brain can reflect these four elements as the compensatory reaction in response to stressful stimuli [69]. The brain activation between the prefrontal region and the visual system may reflect the first two elements through stress detection and emotional response. The top-down processing within the fronto-parietal network provides cognitive input during the situational appraisal. It regulates information based on internal resources and external cues such as the person's perspective of the social cues to execute goal-directed behaviours. In low resilient individuals, these changes can be maladaptive to the brain and result in reduced information processing efficiency [87].

The current work implemented a static-based EC analyses where the PSI metric was averaged across 1-minute segments of brain activity. The role of time on the neurobiology of resilience [18] has shown that the brain reacts to stressful stimuli within seconds and continues to adapt/maladapt across minutes and days. Graph-theory metric of dynamic cognitive flexibility has also shown stronger correlation with resilience scores, compared to its static-based measure [48]. We postulate that the role of static and dynamic EEG features are both equally important since mental resilience is present with and without the presence of stimulus. The similarity or differences between these two feature-types may also provide evidence in the debate between static and dynamic resilience, where the former characterizes it as a personality trait whilst the latter defines it as an adaptation process.

The dominance of a particular brain rhythms was not observed in any of the CE, OE and Task conditions. The EC features selected as predictors spread across delta to gamma brainwaves (as illustrated in Fig. 6). In our previous work using graph theory features [88], the global network metrics selected as predictors to classify mental resilience were largely from alpha to beta3 brainwaves. The relevance of each brainwaves to mental resilience have also been observed in previous literature. Delta, alpha and beta brainwaves were negatively correlated to resilience scores during resting in healthy cohort [48]. Similarly, cross-spectra of the beta brainwaves were negatively correlated with resiliency in traumatized patients [89]. In an analysis that purposively compared the performance of network measures based on frequency bands, Aydin observed that full-band features achieved the highest deep learning accuracy in classifying two groups of emotional regulation strategies, followed by the beta-band features [70]. The importance of EC features across the broad frequency bands may be highlighting the exchange of information between the subconscious mind (i.e., internal resource) and the goal-directed behaviour driving mental resilience.

Findings of this study were based on EEG data from healthy adults who were mostly between 20-30 years old. These findings may differ in different populations due to the differences in cognitive and socio-economic resources [90]. Factors such as the working industries, job scope, and salary that contribute to one's socio-economic status during his/her adulthood may influence the psychosocial factors of resilience such as coping mechanism and social support. Highly resilient children with low socio-economic status who were frequently exposed to threats had better control in adapting the dynamic connectivity between the anterior default mode network and right central executive network, which reflected better internal processing of stimuli [91]. This was similarly observed in resilient adults where their modulation of brain activations between prefrontal cortex and amygdala indicated better cognitive appraisal [20]. These indirect factors of resilience vary across demography and personalities. To curb the variability issue, we opted for a psychological instrument that can measure general resilience (direct assessment) and have been proven to be reliable across different populations. The choice of CD-RISC instrument to extract the ground truth label was made to help in strengthening the generalizability of our findings since this instrument has high reliability findings across age and culture [6], [32].

This study implemented a decision-level fusion approach from three different mental conditions to detect low mental resilience using EEG-EC features. This study reports as a validating analysis to test our mental resilience assessment system using EEG in working adults. Since mental resilience is a dynamic mechanism which can change based on internal and external factors, a physiological-based detection system can provide a more robust assessment on situations that may promote or impede mental resilience. The system can be placed in different work settings with customized work task to assess real-time mental resilience. This assistive tool may be beneficial for working adults exposed to highly stressful work environment such as nurses [5], teachers [23], flight crews [92] and the military [93].

D. DEPLOYMENT PATHWAY

We have built a software coined as RASMi (Resilience Assessment System using Mind) where the user can upload their EEG signals into the software. The software will then process the signals and predict the resilience level of the user. Fig. 10 illustrates a sample of our graphic user interface. The current work has achieved TRL 5 where it has been tested with data collected from an actual working environment, the early childhood centre. The plan for deployment is to approach the human resources from different industries to promote the idea of a brain-based resilience assessment as a mental health tool for their employees. The software will be deployed following the Malaysian Medical Council confidentiality guideline, Personal Data Protection Act, and the health privacy guideline employed by the particular stakeholders. Prior to usage, user will be prompted on the privacy that entails, and what information will be revealed to the employer. The RASMi can be deployed at resting or during a work routine which can be delivered in an actual or virtual setting that emulates the working environment. A report will be generated for the user.

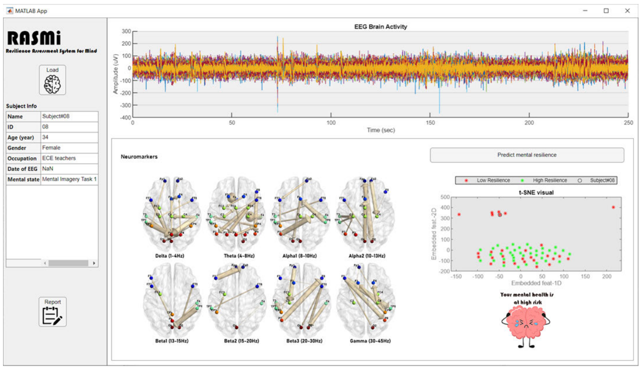

FIGURE 10. User interface for the RASMi software.

E. LIMITATIONS AND FUTURE DIRECTIONS

While our findings reported good performance of EEG-resilience model, there are some limitations in the current study which we outlined here as directions for future studies. Although the classification model achieved performance $> 80\%$, the framework can be further improved with a larger sample size. A robust EEG model relies on a large number of data with heterogenous sample to ensure model generalization. The number of participants recruited in this study was based on the optimal sample size estimated using power analysis. Increasing the sample size would allow for a larger training/test split to evaluate the classification model. In addition, the performance observed in CE and EO conditions were poorer than the task. The use of dynamic features may help detect temporal changes of brain activity and improve the detection of mental resilience neuromarkers during resting conditions. Future study should also consider the use of dynamic functional/effective connectivity analysis.

Moreover, the current neuromarkers were identified from CSD topographies where relatively local and radial sources are emphasized whilst spatially broad activities are attenuated. On the other hand, source-space method applies a head-mathematical model and inverse algorithm to estimate the deeper brain sources. It provides higher spatial resolution to identify deeper brain activity with higher computational complexity such as choices of algorithm, and head template. With more resources, the implementation of source-space localization may reveal important brain networks in the deeper regions that has been observed on the neurobiological level. A combination of both localization methods will corroborate brain connectivity truly associated with mental resilience and minimize the variability in findings due to volume conduction and non-unique solutions.

V. CONCLUSION

The current work demonstrates the potential of fusing EEG-features from different mental conditions to assess mental resilience of healthy subjects. Spectra, FC and EC were compared to identify features with the highest performance in predicting resilience scores at resting and task conditions. The comparison among regression models reveals the EC as the most promising neuromarkers in assessing mental resilience. Its consistent performance in both resting and task models suggests that mental resilience is highly dependent on the directional flow of brain activity between regions. Moreover, the fusion of decisions from CE, EO and task conditions improved the classification performance in assessing low and high mental resilience. Thus, the proposed system has the potential of assisting in mental resilience assessment in workplace settings.

ACKNOWLEDGMENT

The authors would like to thank Mazlina Che Mustafa and Masayu Dzainudin from the National Child Development Research Centre, University Pendidikan Sultan Idris; and Choong Cheok Xuan from Universiti Teknologi PETRONAS for their assistance in data collection.

REFERENCES

[1] J. Ellery, "Integrating salutogenesis into wellness in every stage of life [letter to the editor]," *Prev Chronic Dis.*, vol. 18, no. 9, p. 73, Sep. 2021.

[2] Z.-F. Yao and S. Hsieh, "Neurocognitive mechanism of human resilience: A conceptual framework and empirical review," *Int. J. Environ. Res. Public Health*, vol. 16, no. 24, p. 5123, Dec. 2019.

[3] A. Sood, K. Prasad, D. Schroeder, and P. Varkey, "Stress management and resilience training among department of medicine faculty: A pilot randomized clinical trial," *J. Gen. Internal Med.*, vol. 26, no. 8, pp. 858–861, Aug. 2011.

[4] L. Napier and R. K. Bufford, "Effect of solution-focused therapy on resilience in athletes: An EEG study," Ph.D. thesis, Graduate School Clin. Psychol., George Fox Univ., Newberg, OR, USA, 2021.

[5] M. A. Perry et al., "Study protocol for a two-center test of a nurse-implemented chronotherapeutic restoring bundle in critically ill children: RESTORE resilience (R2)," *Contemp. Clin. Trials Commun.*, vol. 23, Sep. 2021, Art. no. 100840.

[6] G. Windle, K. M. Bennett, and J. Noyes, "A methodological review of resilience measurement scales," *Health Quality Life Outcomes*, vol. 9, no. 1, p. 8, Feb. 2011.

[7] C. E. Waugh and E. H. W. Koster, "A resilience framework for promoting stable remission from depression," *Clin. Psychol. Rev.*, vol. 41, pp. 49–60, Nov. 2015.

[8] S. Kuldas and M. Foody, "Neither resiliency-trait nor resilience-state: Transactional resiliency/e," *Youth Soc.*, vol. 54, no. 8, pp. 1352–1376, Jul. 2021.

[9] K. M. Connor and J. R. T. Davidson, "Development of a new resilience scale: The connor-davidson resilience scale (CD-RISC)," *Depression Anxiety*, vol. 18, no. 2, pp. 76–82, Sep. 2003.

[10] O. Friborg, O. Hjemdal, J. H. Rosenvinge, and M. Martinussen, "A new rating scale for adult resilience: What are the central protective resources behind healthy adjustment?" *Int. J. Methods Psychiatric Res.*, vol. 12, no. 2, pp. 65–76, Jun. 2003.

[11] A. S. Masten, "Ordinary magic: Resilience processes in development," *Amer. Psychologist*, vol. 56, no. 3, pp. 227–238, 2001.

[12] A. S. Masten, C. M. Lucke, K. M. Nelson, and I. C. Stallworthy, "Resilience in development and psychopathology: Multisystem perspectives," *Annu. Rev. Clin. Psychol.*, vol. 17, pp. 521–549, May 2021.

[13] B. S. McEwen, J. D. Gray, and C. Nasca, "Recognizing resilience: Learning from the effects of stress on the brain," *Neurobiol. Stress*, vol. 1, pp. 1–11, Jan. 2015.

[14] N. E. Holz, H. Tost, and A. Meyer-Lindenberg, "Resilience and the brain: A key role for regulatory circuits linked to social stress and support," *Mol. Psychiatry*, vol. 25, no. 2, pp. 379–396, Feb. 2020.

[15] Q. Dai et al., "Psychological resilience is positively correlated with habenula volume," *J. Affect. Disorders*, vol. 365, pp. 178–184, Nov. 2024.

[16] T. B. Franklin, B. J. Saab, and I. M. Mansuy, "Neural mechanisms of stress resilience and vulnerability," *Neuron*, vol. 75, no. 5, pp. 747–761, Sep. 2012.

[17] N. P. Daskalakis, R. C. Bagot, K. J. Parker, C. H. Vinkers, and E. R. de Kloet, "The three-hit concept of vulnerability and resilience: Toward understanding adaptation to early-life adversity outcome," *Psychoneuroendocrinology*, vol. 38, no. 9, pp. 1858–1873, Sep. 2013.

[18] N. Watanabe and M. Takeda, "Neurophysiological dynamics for psychological resilience: A view from the temporal axis," *Neurosci. Res.*, vol. 175, pp. 53–61, Feb. 2022.

[19] S. J. A. van der Werff, S. M. van den Berg, J. N. Pannekoek, B. M. Elzinga, and N. J. A. van der Wee, "Neuroimaging resilience to stress: A review," *Frontiers Behav. Neurosci.*, vol. 7, p. 39, May 2013.

[20] A. Feder, S. Fred-Torres, S. M. Southwick, and D. S. Charney, "The biology of human resilience: Opportunities for enhancing resilience across the life span," *Biol. Psychiatry*, vol. 86, no. 6, pp. 443–453, Sep. 2019.

[21] S. Prince-Embury, D. H. Saklofske, and A. K. Vesely, "Measures of resiliency," in *Measures of Personality and Social Psychological Constructs*. Amsterdam, The Netherlands: Elsevier, 2015, pp. 290–321.

[22] J. Hassard, K. R. H. Teoh, G. Visockaite, P. Dewe, and T. Cox, "The cost of work-related stress to society: A systematic review," *J. Occupational Health Psychol.*, vol. 23, no. 1, pp. 1–17, Jan. 2018.

[23] R. Abu Hasan et al., "Resilience-building for mental health among early childhood educators: A systematic review and pilot-study towards an EEG-VR resilience building intervention," *Int. J. Environ. Res. Public Health*, vol. 19, no. 7, p. 4413, Apr. 2022.

[24] T. Jiang, Y. Fang, N. Zheng, and J. Chen, "Understanding construction workers' cognitive processes under risky scenarios through electroencephalography," *Autom. Construction*, vol. 166, Oct. 2024, Art. no. 105674.

[25] J. Góral-Pólrola, E. Kochańska, K. Cielebąk, and M. Pąchalska, "A new, neuromarker-based, form of combined neurofeedback EEG/tDCS training in the reduction of occupational burnout syndrome in an anaesthetic nurse working with COVID-19 patients," *Acta Neuropsychologica*, vol. 22, no. 3, pp. 301–330, Jun. 2024.

[26] B. Patangia, J. M. Rithani, and T. Alfonso, "Application of neuroscience methods in HRDM for brain-based human capital optimization," in *Cognitive Behavioral Neuroscience in Organizational Settings*. Hershey, PA, USA: IGI Global, 2024, pp. 227–261.

[27] H. Huang, H. Hu, F. Xu, Z. Zhang, and J. Yang, "Electroencephalography-based assessment of worker vigilance for evaluating safety interventions in construction," *Adv. Eng. Informat.*, vol. 64, Mar. 2025, Art. no. 102973.

[28] M. Hamada, B. B. Zaidan, and A. A. Zaidan, "A systematic review for human EEG brain signals based emotion classification, feature extraction, brain condition, group comparison," *J. Med. Syst.*, vol. 42, no. 9, p. 162, Sep. 2018.

[29] S. A. Varga and R. Sherman, "Resiliency and functional neurophysiology in emotional regulation as shown by EEG measures," Ph. D. thesis, Saybrook University, Oakland, CA, USA, 2019.

[30] K. KeunhoYoo et al., "Power spectral analysis of resting-state EEG to monitor psychological resilience to stress," *Psychiatry Res. Commun.*, vol. 4, no. 3, Sep. 2024, Art. no. 100175.

[31] P. Mathews, *Sample Size Calculations: Practical Methods for Engineers and Scientists*. Fairport Harbor, OH, USA: Mathews Malnar and Bailey, Inc, 2010.

[32] J. R. Davidson. (2020). *Connor-davidson Resilience Scale (CD-RISC) Manual.* [Online]. Available: www.connordavidson-resiliencescale.com/

[33] M. W. Lipsey and D. B. Wilson, *Practical Meta-analysis: The Effect Size* (Applied social research methods series), vol. 49. Newbury Park, CA, USA: Sage, 2001.

[34] K. L. Lopez, A. D. Monachino, S. Morales, S. C. Leach, M. E. Bowers, and L. J. Gabard-Durnam, "HAPPILEE: HAPPE in low electrode electroencephalography, a standardized pre-processing software for lower density recordings," *NeuroImage*, vol. 260, Oct. 2022, Art. no. 119390.

[35] L. Pion-Tonachini, K. Kreutz-Delgado, and S. Makeig, "ICLabel: An automated electroencephalographic independent component classifier, dataset, and website," *NeuroImage*, vol. 198, pp. 181–197, Sep. 2019.

[36] C. E. Tenke and J. Kayser, "Generator localization by current source density (CSD): Implications of volume conduction and field closure at intracranial and scalp resolutions," *Clin. Neurophysiol.*, vol. 123, no. 12, pp. 2328–2345, Dec. 2012.

[37] M. X. Cohen, *Analyzing Neural Time Series Data: Theory and Practice*. Cambridge, MA, USA: MIT Press, 2014.

[38] B. Burle, L. Spieser, C. Roger, L. Casini, T. Hasbroucq, and F. Vidal, "Spatial and temporal resolutions of EEG: Is it really black and white? A scalp current density view," *Int. J. Psychophysiology*, vol. 97, no. 3, pp. 210–220, Sep. 2015.

[39] C. Kamarajan, A. K. Pandey, D. B. Chorlian, and B. Porjesz, "The use of current source density as electrophysiological correlates in neuropsychiatric disorders: A review of human studies," *Int. J. Psychophysiology*, vol. 97, no. 3, pp. 310–322, Sep. 2015.

[40] F. Perrin, J. Pernier, O. Bertrand, and J. F. Echallier, "Spherical splines for scalp potential and current density mapping," *Electroencephalogr. Clin. Neurophysiology*, vol. 72, no. 2, pp. 184–187, Feb. 1989.

[41] L. Hu and Z. Zhang, *EEG Signal Processing and Feature Extraction*. Singapore: Springer, 2019.

[42] R. Vallat. (2018). *Compute the Average Bandpower of an EEG Signal*. [Online]. Available: https://raphaelvallat.com/bandpower.html

[43] A. Angelidis, M. Hagenaars, D. van Son, W. van der Does, and P. Putman, "Do not look away! Spontaneous frontal EEG theta/beta ratio as a marker for cognitive control over attention to mild and high threat," *Biol. Psychol.*, vol. 135, pp. 8–17, May 2018.

[44] J.-P. Lachaux, E. Rodriguez, J. Martinerie, and F. J. Varela, "Measuring phase synchrony in brain signals," *Human Brain Mapping*, vol. 8, no. 4, pp. 194–208, 1999.

[45] L. L. Gollo, C. Mirasso, O. Sporns, and M. Breakspear, "Mechanisms of zero-lag synchronization in cortical motifs," *PLoS Comput. Biol.*, vol. 10, no. 4, Apr. 2014, Art. no. e1003548.

[46] W. Jian, M. Chen, and D. J. McFarland, "EEG based zero-phase phase-locking value (PLV) and effects of spatial filtering during actual movement," *Brain Res. Bull.*, vol. 130, pp. 156–164, Apr. 2017.

[47] B. T. Schmidt, A. S. Ghuman, and T. J. Huppert, "Whole brain functional connectivity using phase locking measures of resting state magnetoencephalography," *Frontiers Neurosci.*, vol. 8, no. 141, pp. 1–15, Jun. 2014.

[48] V. Paban, J. Modolo, A. Mheich, and M. Hassan, "Psychological resilience correlates with EEG source-space brain network flexibility," *Netw. Neurosci.*, vol. 3, no. 2, pp. 539–550, Jan. 2019.

[49] J.-P. Lachaux, E. Rodriguez, M. Le Van Quyen, A. Lutz, J. Martinerie, and F. J. Varela, "Studying single-trials of phase synchronous activity in the brain," *Int. J. Bifurcation Chaos*, vol. 10, no. 10, pp. 2429–2439, Oct. 2000.

[50] A. M. Bastos and J.-M. Schoffelen, "A tutorial review of functional connectivity analysis methods and their interpretational pitfalls," *Frontiers Syst. Neurosci.*, vol. 9, p. 175, Jan. 2016.

[51] G. Nolte, A. Ziehe, N. Krämer, F. Popescu, and K. Müller, "Comparison of Granger causality and phase slope index," in *Proc. Workshop Causality, Objectives Assessment NIPS*, Dec. 2008, pp. 267–276.

[52] S. Haufe, V. V. Nikulin, K.-R. Müller, and G. Nolte, "A critical assessment of connectivity measures for EEG data: A simulation study," *NeuroImage*, vol. 64, pp. 120–133, Jan. 2013.

[53] M. J. Silfverhuth, H. Hintsala, J. Kortelainen, and T. Seppänen, "Experimental comparison of connectivity measures with simulated EEG signals," *Med. Biol. Eng. Comput.*, vol. 50, no. 7, pp. 683–688, Jul. 2012.

[54] G. Nolt et al. (2008). *Phase Slope Index*. [Online]. Available: http://doc.ml.tu-berlin.de/causality/

[55] G. Niso et al., "HERMES: Towards an integrated toolbox to characterize functional and effective brain connectivity," *Neuroinformatics*, vol. 11, no. 4, pp. 405–434, Oct. 2013.

[56] M. Rubinov and O. Sporns, "Complex network measures of brain connectivity: Uses and interpretations," *NeuroImage*, vol. 52, no. 3, pp. 1059–1069, Sep. 2010.

[57] C. Leys, C. Ley, O. Klein, P. Bernard, and L. Licata, "Detecting outliers: Do not use standard deviation around the mean, use absolute deviation around the median," *J. Experim. Social Psychol.*, vol. 49, no. 4, pp. 764–766, Jul. 2013.

[58] K. Schultebraucks and I. R. Galatzer-Levy, "Machine learning for prediction of posttraumatic stress and resilience following trauma: An overview of basic concepts and recent advances," *J. Traumatic Stress*, vol. 32, no. 2, pp. 215–225, Apr. 2019.

[59] M. M. van der Miesen, M. A. Lindquist, and T. D. Wager, "Neuroimaging-based biomarkers for pain: State of the field and current directions," *PAIN Rep.*, vol. 4, no. 4, p. e751, 2019.

[60] F. M. Al-Shargie, O. Hassanin, U. Tariq, and H. Al-Nashash, "EEG-based semantic vigilance level classification using directed connectivity patterns and graph theory analysis," *IEEE Access*, vol. 8, pp. 115941–115956, 2020.

[61] R. Kalisch, M. B. Müller, and O. Tüscher, "A conceptual framework for the neurobiological study of resilience," *Behav. Brain Sci.*, vol. 38, no. e92, pp. 1–79, 2015.

[62] M. A. Rahman, M. S. B. Yusoff, N. S. Roslan, J. A.-M. Mohammad, and A. Ahmad, "Development and validation of the medical professionals resilience scale," *BMC Health Services Res.*, vol. 21, no. 1, p. 482, Dec. 2021.

[63] W. J. Curtis and D. Cicchetti, "Emotion and resilience: A multilevel investigation of hemispheric electroencephalogram asymmetry and emotion regulation in maltreated and nonmaltreated children," *Develop. Psychopathology*, vol. 19, no. 3, pp. 811–840, Jun. 2007.

[64] T. Cevada, A. Moreira, L. M. P. Vilete, V. Oertel-Knöchel, and A. C. Deslandes, "Resilience, psychological characteristics, and resting-state brain cortical activity in athletes and non-athletes," *Open Sports Sci. J.*, vol. 13, no. 1, pp. 86–96, Oct. 2020.

[65] R. C. Vergara, C. Moënne-Loccoz, C. Ávalos, J. Egaña, and P. E. Maldonado, "Finger temperature: A psychophysiological assessment of the attentional state," *Frontiers Hum. Neurosci.*, vol. 13, no. 66, pp. 1–13, Mar. 2019.

[66] N. Levit-Binnun and Y. Golland, "Adding network approaches to a neurobiological framework of resilience," *Behav. Brain Sci.*, vol. 38, p. 111, 2015.

[67] M. Zhang et al., "Randomized EEG functional brain networks in major depressive disorders with greater resilience and lower rich-club coefficient," *Clin. Neurophysiol.*, vol. 129, no. 4, pp. 743–758, Apr. 2018.

[68] F. Duan et al., "Topological network analysis of early Alzheimer's disease based on resting-state EEG," *IEEE Trans. Neural Syst. Rehabil. Eng.*, vol. 28, no. 10, pp. 2164–2172, Oct. 2020.

[69] G. Jauny, F. Eustache, and T. T. Hinault, "M/EEG dynamics underlying reserve, resilience, and maintenance in aging: A review," *Frontiers Psychol.*, vol. 13, no. 861973, pp. 1–13, May 2022.

[70] S. Aydın, "Investigation of global brain dynamics depending on emotion regulation strategies indicated by graph theoretical brain network measures at system level," *Cognit. Neurodynamics*, vol. 17, no. 2, pp. 331–344, Apr. 2023.

[71] M. H. Teicher, J. A. Samson, C. M. Anderson, and K. Ohashi, "The effects of childhood maltreatment on brain structure, function and connectivity," *Nature Rev. Neurosci.*, vol. 17, no. 10, pp. 652–666, Oct. 2016.

[72] X. Geng, J. Xu, B. Liu, and Y. Shi, "Multivariate classification of major depressive disorder using the effective connectivity and functional connectivity," *Frontiers Neurosci.*, vol. 12, no. 38, pp. 1–16, Feb. 2018.

[73] R. W. Thatcher, E. Palmero-Soler, D. M. North, and C. J. Biver, "Intelligence and EEG measures of information flow: Efficiency and homeostatic neuroplasticity," *Sci. Rep.*, vol. 6, no. 1, p. 38890, Dec. 2016.

[74] C. Gómez et al., "Assessment of EEG connectivity patterns in mild cognitive impairment using phase slope index," in *Proc. 40th Annu. Int. Conf. IEEE Eng. Med. Biol. Soc. (EMBC)*, Jul. 2018, pp. 263–266.

[75] R. Khosrowabadi, "Stress and perception of emotional stimuli: Long-term stress rewiring the brain," *Basic Clin. Neurosci. J.*, vol. 9, no. 2, pp. 107–120, Mar. 2018.

[76] E. van Diessen et al., "Opportunities and methodological challenges in EEG and MEG resting state functional brain network research," *Clin. Neurophysiol.*, vol. 126, no. 8, pp. 1468–1481, Aug. 2015.

[77] E. Mezzacappa, B. B. Brown, and M. J. Prinstein, "Executive function," in *Encyclopedia of Adolescence*. Washington, DC, USA: National Academy Press, 2011, pp. 142–150.

[78] M. Göttlich, U. M. Krämer, A. Kordon, F. Hohagen, and B. Zurowski, "Decreased limbic and increased fronto-parietal connectivity in unmedicated patients with obsessive-compulsive disorder," *Human Brain Mapping*, vol. 35, no. 11, pp. 5617–5632, Nov. 2014.

[79] K. L. Lopez, A. D. Monachino, K. M. Vincent, F. C. Peck, and L. J. Gabard-Durnam, "Stability, change, and reliable individual differences in electroencephalography measures: A lifespan perspective on progress and opportunities," *NeuroImage*, vol. 275, Jul. 2023, Art. no. 120116.

[80] F. I. Mouri, C. E. Valderrama, and S. G. Camorlinga, "Identifying relevant asymmetry features of EEG for emotion processing," *Frontiers Psychol.*, vol. 14, pp. 1–15, Aug. 2023.

[81] S. Gupta and J. Reddy, "EEG signatures of resilience across individuals with high and low anxiety," *NeuroRegulation*, vol. 12, no. 1, pp. 12–28, Mar. 2025.

[82] A.-M. Brouwer, Neerincx, V. Kallen, L. V. D. Leer, and M. T. Brinke, "EEG alpha asymmetry, heart rate variability and cortisol in response to virtual reality induced stress," *J. Cybertherapy Rehabil.*, vol. 4, no. 1, pp. 27–56, 2011.

[83] L. Shi, J. Sun, D. Wei, and J. Qiu, "Recover from the adversity: Functional connectivity basis of psychological resilience," *Neuropsychologia*, vol. 122, pp. 20–27, Jan. 2019.

[84] D. Samson, I. A. Apperly, C. Chiavarino, and G. W. Humphreys, "Left temporoparietal junction is necessary for representing someone else's belief," *Nature Neurosci.*, vol. 7, no. 5, pp. 499–500, May 2004.

[85] J. J. Geng and S. Vossel, "Re-evaluating the role of TPJ in attentional control: Contextual updating?" *Neurosci. Biobehavioral Rev.*, vol. 37, no. 10, pp. 2608–2620, Dec. 2013.

[86] R. E. Smith and J. C. Ascough, *Promoting Emotional Resilience: Cognitive-Affective Stress Management Training*. New York, NY, USA: The Guilford Press, 2016.

[87] S. R. Kesler et al., "Altered functional brain connectivity, efficiency, and information flow associated with brain fog after mild to moderate COVID-19 infection," *Sci. Rep.*, vol. 14, no. 1, p. 22094, Sep. 2024.

[88] A. Siddiqui, R. Abu Hasan, S. Saad Azhar Ali, I. Elamvazuthi, C.-K. Lu, and T. B. Tang, "Detection of low resilience using data-driven effective connectivity measures," *IEEE Trans. Neural Syst. Rehabil. Eng.*, vol. 32, pp. 3657–3668, 2024.

[89] M. Brunetti et al., "Resilience and cross-network connectivity: A neural model for post-trauma survival," *Prog. Neuro-Psychopharmacology Biol. Psychiatry*, vol. 77, pp. 110–119, Jul. 2017.

[90] K. E. Riehm et al., "Association between psychological resilience and changes in mental distress during the COVID-19 pandemic," *J. Affect. Disorders*, vol. 282, pp. 381–385, Mar. 2021.

[91] S. Eaton, H. Cornwell, C. Hamilton-Giachritsis, and G. Fairchild, "Resilience and young people's brain structure, function and connectivity: A systematic review," *Neurosci. Biobehavioral Rev.*, vol. 132, pp. 936–956, Jan. 2022.

[92] B. Bennett, "Neurofeedback and expeditionary training paradigms for developing innate resilience in exploration-class crew," in *Proc. ASCEND*, Nov. 2020, pp. 1–13.

[93] R. Stevens, T. Galloway, J. Lamb, R. Steed, and C. Lamb, "Team resilience: A neurodynamic perspective," in *Foundations of Augmented Cognition*. Cham, Switzerland: Springer, 2015, pp. 336–347.